Supporting Information for

Differential dimerization of variants in the NR2E3 ligand-binding domain linked to enhanced S-Cone Sensitivity Syndrome (ESCS)

Désirée von Alpen, H. Viet Tran, Nicolas Guex, Giulia Venturini, Francis L. Munier, Daniel F. Schorderet, Neena B. Haider, and Pascal Escher

Table of contents

A

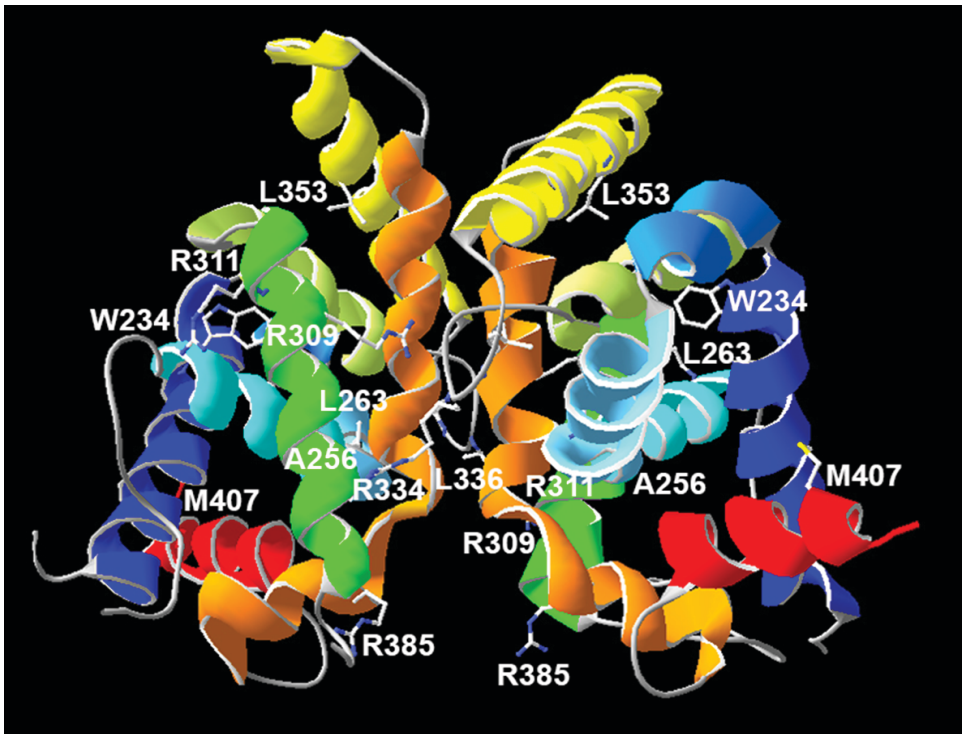

B

```
                                                                    h3
HHFMASLITA ETCAKLEPED ADENIDVTSN DPEFPSSPYS SSSPCGLDSI HETSARLLFM 230
    h3      h3‘          h4              h5
AVKWAKNLPV FSSLPFRDQV ILLEEAWSEL FLLGAIQWSL PLDSCPLLAP PEASAAGGAQ 290
              h7                    h8                    h9
GRLTLASMET RVLQETISRF RALAVDPTEF ACMKALVLFK PETRGLKDPE HVEALQDQSQ 350
  h9                      h10/h11                    h12(AF2)
VMLSQHSKAH HPSQPVRFGK LLLLLPSLRF ITAERIELLF FRKTIGNTPM EKLLCDMFKN 410
```

Supp. Figure S1. Structural analysis of the NR2E3 LBD.

A) NR2E3 LBD homodimer crystal structure in an autorepressed conformation (PDB_4LOG), spanning helices 3 and 3’ (dark blue), 4 (blue), 5 (light blue), 7 (green), 8 (lime green), 9 (yellow), 10/11 (orange) and 12 (red) (Tan et al., 2013). Variant residues analyzed in this study are indicated with their side chains to facilitate localization.

B) Primary structure of the C-terminus of the hinge region and LBD of the human NR2E3 protein (amino acids 171-410). Color shading is according to panel A and residues point-mutated in human patients are shown in red (see also Supp. Table S2). Residues 283 to 287 were not solved by X-ray crystallography.

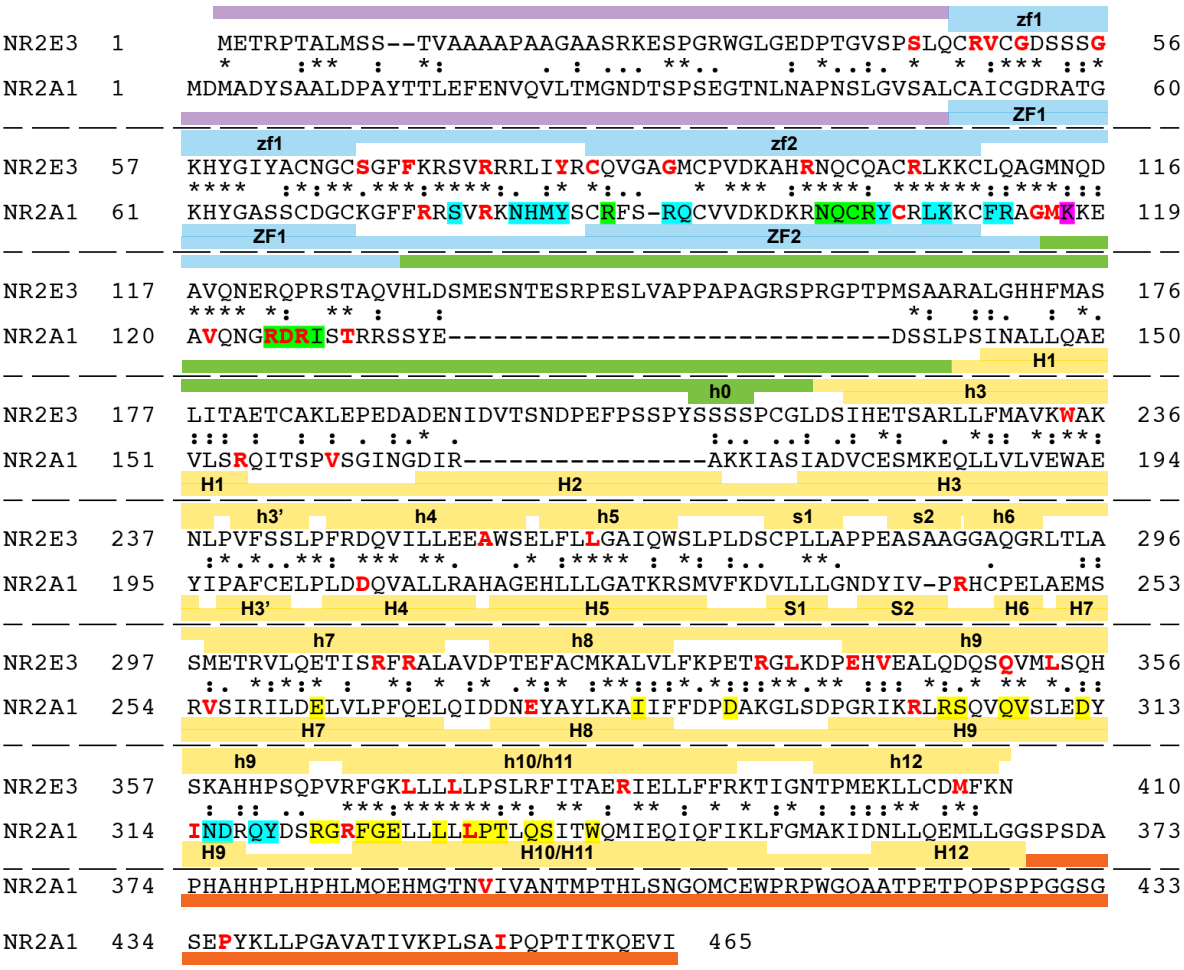

Supp. Figure S2. Sequence homology between NR2E3 (PNR) and NR2A1 (HNF4α). Human NR2E3 (SwissProt_Q9Y5X4, 410 aa) and human NR2A1 (SwissProt_B6ZGT3, 465 aa) amino acid sequences were aligned with Clustal W (www.ebi.ac.uk/Tools/msa/clustalw), and, in parallel, aligned with Clustal Omega (www.ebi.ac.uk/Tools/msa/clustalo). Finally, the alignment was manually curated. Structural domains are indicated as colored bars along the sequences: A/B domain in purple, DBD in blue, hinge in green, LBD in yellow, and F domain in red. Observed or predicted α-helices (h, H) and β-sheets (s, S) are indicated in lower case for NR2E3 and in upper case for NR2A1. For NR2A1, LBD/LBD interactions are highlighted in yellow, LBD/DBD interactions in turquoise, hinge/DBD interactions in green, and hinge/LBD interactions in purple. Localization of mutant residues is indicated in red.

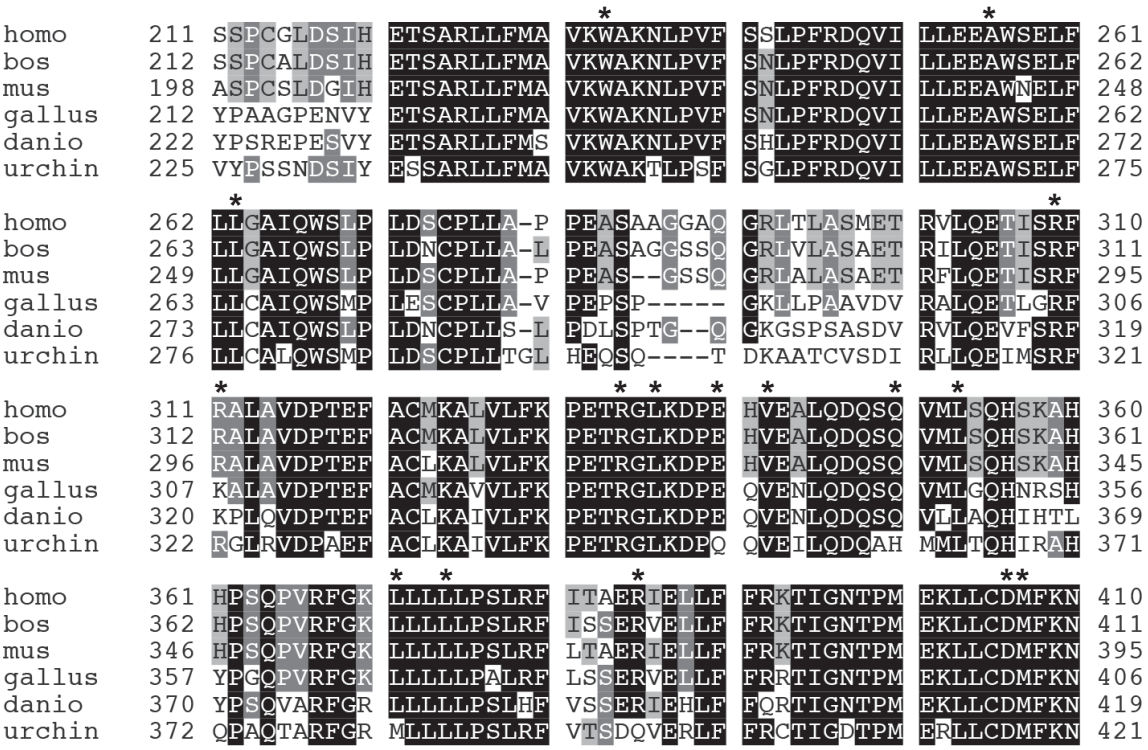

Supp. Figure S3. Evolutionary conservation of the NR2E3 ligand-binding domain (LBD). Human (homo sapiens), bovine (bos taurus), murine (mus musculus), chicken (gallus gallus), zebrafish (danio rerio) and sea urchin (strongylocentrotus purpuratus) sequences were aligned with Clustal Omega (www.ebi.ac.uk/Tools/msa/clustalo) and visualized with WAVis (wavis.img.cas.cz). Amino acid numbering is given on each line and single nucleotide variants found in human patients are indicated by stars.

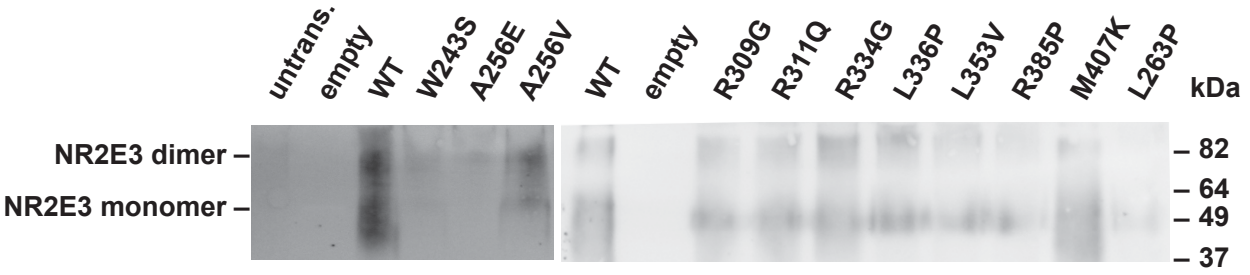

Supp. Figure S4. Non-denaturing gel electrophoresis of NR2E3. Wild-type (wt) and mutant NR2E3 proteins were separated on an 8% non-denaturing polyacrylamide gel and transferred on membrane for Western blotting with a rabbit polyclonal antibody directed against the central region of NR2E3. Untransfected HEK293T cells (untrans.) and cells transfected with an empty pcDNA3.1-HisC vector (empty) were used as negative control. The NR2E3 monomer migrates at ~49 kDa and the NR2E3 dimer above 82 kDa. Representative lanes of two out of 4 gels are shown.

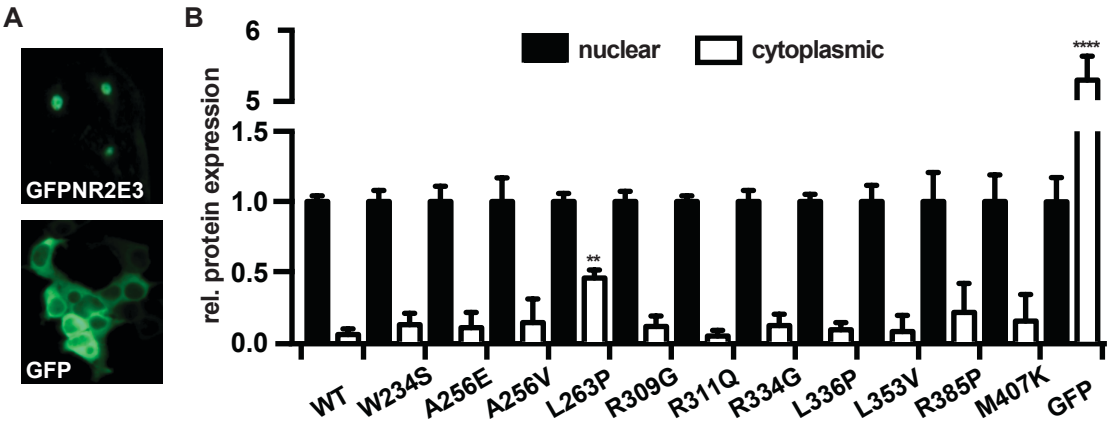

Supp. Figure S5. Cellular localization of NR2E3.

A) Fluorescence imaging showed nuclear localization of NR2E3 fused to GFP (GFPNR2E3) in transiently transfected HEK293T cells (upper panel), in contrast to a cytoplasmic localization of GFP alone (lower panel).

B) Quantification of relative (rel.) nuclear (black bar) and cytoplasmic (white bar) protein expression as assessed by Western Blot. Quantification was performed on four experiments, nuclear expression of each experimental condition set to 1 and SEM indicated. For statistical analysis, ordinary one-way ANOVA with Dunnett's multiple comparison test was performed, comparing nuclear protein expression levels of wild-type NR2E3 (WT) to the different variants. GFP alone was predominantly expressed in the cytoplasm. **: $p<0.01$; ****: $p<0.0001$.

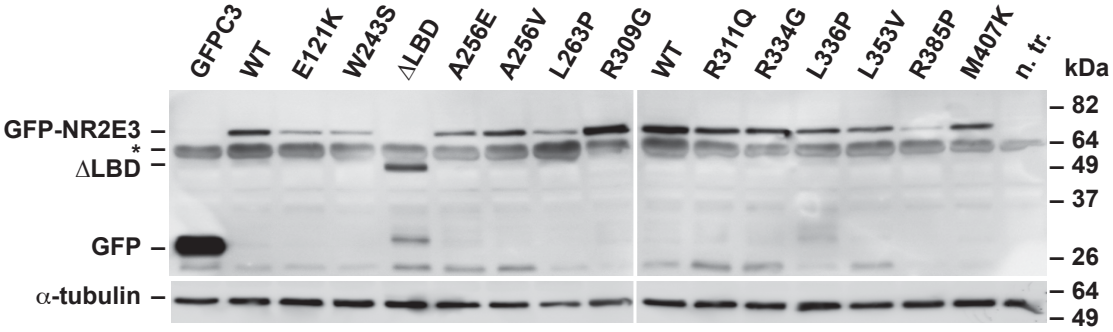

Supp. Figure S6. Expression of NR2E3-GFP fusion proteins. HEK293T cells were transfected with GFPC3 and, wild-type and variant NR2E3-GFPC3 BRET^2 expression vectors (upper panel). n. tr.: non transfected. Asterisk denotes a non-specific signal. Equal loading was assessed with probing the membrane for α-tubulin expression (lower panel). Note the decreased size of the truncated NR2E3-p.W234X protein (ΔLBD).

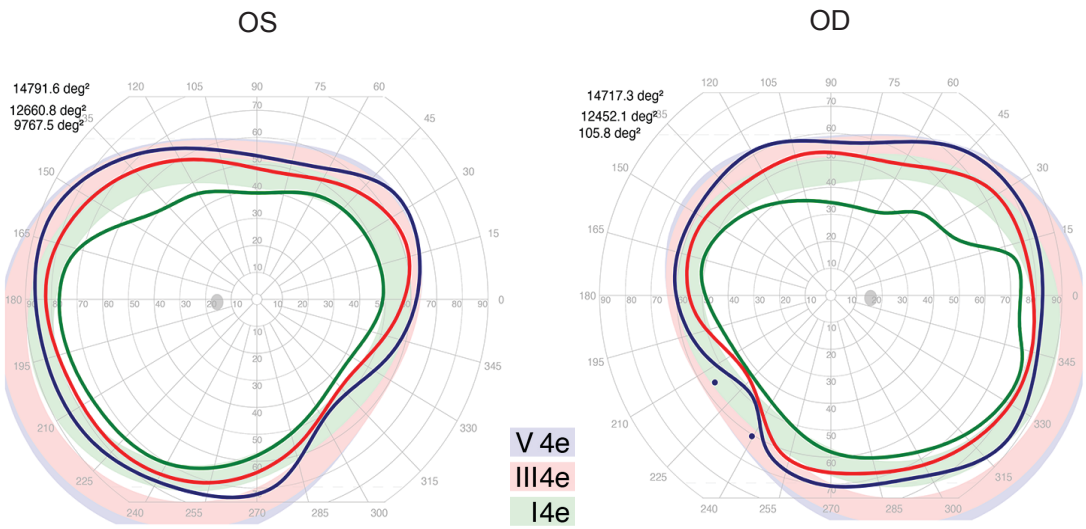

Supp. Figure S7. Visual field measurements of patient II.I. Dynamic perimetry on an Octopus 900 perimeter showed a bilateral slight supero-temporal dissociation of isopter V4e and IVe but were otherwise physiologic. Isopter V4e is in blue, III4e in red, and I4e in green.

Supp. Table S1. Primer Sequences

Construct	forward primer (5'-3')	reverse primer (5'-3')
E121K	GACGCCGTGCAGAACAAGCGCCAGCCGCGAAG	CTTCGCGGCTGGCGCTTGTTCTGCACGGCGTC
W234S	CATGGCCGTCAAGTCGGCCAAGAACCTG	CAGGTTCTTGGCCGACTTGACGGCCATG
W234X	CATGGCCGTCAAGTAGGCCAAGAACCTG	CAGGTTCTTGGCCTACTTGACGGCCATG
A256E	CCTGCTGGAAGAGGAGTGGAGTGAACTCTTTC	GAAAGAGTTCACTCCACTCCTCTTCCAGCAGG
A256V	CCTGCTGGAAGAGGTGTGGAGTGAACTCTTTC	GAAAGAGTTGACTCCACACCTCTTCCAGCAGG
L263P	GTGAACTCTTTCTCCCCGGGGCCATCCAGTG	CACTGGATGGCCCCGGGGAGAAAGAGTTCAC
R309G	CAGGAAACTATCTCTGGGTTCCGGGCATTGG	CCAATGCCCGGAACCCAGAGATAGTTTCCTG
R311Q	CCTGCAGGAAACTATCTCTCGGTTCCAGGCATTGGCGG	CCGCCAATGCCTGGAACCGAGAGATAGTTTCCTGCAGG
R334G	CTTCAAGCCAGAGACGGGGGGCCTGAAGGATC	GATCCTTCAGGCCCCCCGTCTCTGGCTTGAAG
L336P	CAGAGACGCGGGGCCCGAAGGATCCTGAGCAC	GTGCTCAGGATCCTTCGGGCCCCGCGTCTCTG
L353V	CAGTCCCAAGTGATGGTGAGCCAGCACAGCAAG	CTTGCTGTGCTGGCTCACCATCACTTGGGACTG
R385P	GTTTATCACTGCGGAACCCATCGAGCTCCTCTTTTTC	GAAAAAGAGGAGCTCGATGGGTTCCGCAGTGATAAAC
M407K	GAAGCTCCTTTGTGATAAGTTCAAAAACTAGTGGG	CCCACTAGTTTTTGAACTTATCACAAAGGAGCTTC
NRL	GGAAGATCTATGGCCCTGCCCCCCAGCCCC	CGGGGTACCGAGGAAGAGGTGGGAGGGGTC
NRLstop	GGAAGATCTATGGCCCTGCCCCCCAGCCCC	CGGGGTACCTCAGAGGAAGAGGTGGGAGGG
NR1D1	GGACTCGAGTATGACGACCCTGGACTCCAAT	CGGGGTACCCTGGGCGTCCACCCGGAAGGA
NR1D1stop	GGACTCGAGTATGACGACCCTGGACTCCAAT	CGGGGTACCTCACTGGGCGTCCACCCGGAA
NR2E1	GGAAGATCTATGAGCAAGCCAGCCGGATCA	CGGGGTACCGATATCACTGGATTTGTACAT
NR2E1stop	GGAAGATCTATGAGCAAGCCAGCCGGATCA	CGGGGTACCTTAGATATCACTGGATTTGTA
RXRα	GGAAGATCTATGGACACCAAACATTTCCTG	CGGGGTACCAGTCATTTGGTGCGGCGC
RXRαstop	GGAAGATCTATGGACACCAAACATTTCCTG	CGGGGTACCCTAAGTCATTTGGTGCGGCGC

See Materials and Methods section for the use of primers.

Supp. Table S2. Variants in the *NR2E3* gene

Region	DNA sequence change[a]	Protein change[b]	Functional domain	Predicted effect / *in vitro* studies[c]	First description
intron 1	c.119-3C>G	n.d.	n.a.	skipping of exon 2	(Audo, et al., 2008)
intron 1	c.119-2A>C	p.V41Afs*23	n.a.	skipping of exon 2	(Haider, et al., 2000)
exon 2	c.131C>A	p.S44*	AF1	truncated protein	(Khan, et al., 2010)
exon 2	c.142C>T	p.R48C	DBD/zf1	no DNA binding	(Kuniyoshi, et al., 2013)
exon 2	c.143_144del2ins25	p.R48Qfs*66	DBD	truncated protein	(Kannabiran, et al., 2012)
exon 2	c.145G>A	p.V49M	DBD/zf1	no DNA binding	(Audo, et al., 2008)
exon 2	c.151G>A	p.G51R	DBD/zf1	no DNA binding	(Kuniyoshi, et al., 2013)
exon 2	c.166G>A	p.G56R	DBD/zf1	no DNA binding	(Coppieters, et al., 2007)
exon 2	c.194_202del9[a]	p.N65_C67del	DBD	no DNA binding	(Haider, et al., 2000)
exon 2	c.196_201del6	p.G66_C67del	DBD	no DNA binding	(Udar, et al., 2011)
exon 2	c.202A>G	p.S68G	DBD	no DNA binding	(Park, et al., 2013)
exon 2	c.211_213del3	p.F71del	DBD	no DNA binding	(Pachydaki, et al., 2009)
exon 2	c.226C>T	p.R76W	DBD	no DNA binding	(Haider, et al., 2000)
exon 2	c.227G>A	p.R76Q	DBD	no DNA binding	(Haider, et al., 2000)
exon 2	c.242A>G	p.Y81C	DBD	no DNA binding	(Audo, et al., 2008)
exon 3	c.247G>A	p.C83Y	DBD/zf2	no DNA binding	(Rocha-Sousa, et al., 2011)
exon 3	c.263G>T	p.G88V	DBD/zf2	no DNA binding	(Wright, et al., 2004)
exon 3	c.290G>A	p.R97H	DBD/zf2	no DNA binding	(Haider, et al., 2000)
exon 3	c.310C>T	p.R104W	DBD/zf2	no DNA binding	(Haider, et al., 2000)
exon 3	c.311G>A	p.R104Q	DBD/zf2	no DNA binding	(Hayashi, et al., 2005)
exon 4	c.363C>T	p.R125*	DBD	no LBD	(Cassiman, et al., 2013)
exon 4	c.481delA	p.T161Hfs*18	hinge	no LBD	(Wright, et al., 2004)
exon 5	c.701G>A	p.W234S	LBD/h3	impaired repression	(Haider, et al., 2000)
exon 5	c.724_725del2	p.S242Qfs*1	LBD	truncated LBD	(Collin, et al., 2011)
intron 5	c.747+1G>C	n.d.	n.a.	skipping of exon 6	(Bandah, et al., 2009)
exon 6	c.767C>A	p.A256E	LBD/h4		(Sharon, et al., 2003)
exon 6	c.767C>T	p.A256V	LBD/h4		(Lam, et al., 2007)
exon 6	c.788T>C	p.L263P	LBD/h5	no dimerization	(Wright, et al., 2004)
exon 6	c.827_843del17	p.P276Rfs*59	LBD	truncated LBD	(Sharon, et al., 2003)
exon 6	c.925C>G	p.R309G	LBD/h7		(Haider, et al., 2000)
exon 6	c.932G>A	p.R311Q	LBD/h7	impaired repression	(Haider, et al., 2000)
exon 6	c.951delC	p.T318Rfs*6	LBD	truncated LBD	www.lovd.nl/eye
exon 7	c.1000C>G	p.R334G	LBD		(Hayashi, et al., 2005)
exon 7	c.1007T>C	p.L336P	LBD	no dimerization	(Wright, et al., 2004)
exon 7	c.1018G>A	p.E340K[e]	LBD/h9		(Ripamonti, et al., 2014)
exon 7	c.1025T>G	p.V342G	LBD/h9		(Siemiatkowska, et al., 2011)
exon 7	c.1034_1038del5	p.L345Kfs*2	LBD	truncated LBD	(Bernal, et al., 2008)
exon 7	c.1048C>T	p.Q350*	LBD	truncated LBD	(Nakamura, et al., 2004)
exon 7	c.1049A>G	p.Q350R	LBD/h9		(Pachydaki, et al., 2009)
exon 7	c.1057C>G	p.L353V	LBD/h9	no dimerization	(Wright, et al., 2004)
exon 7	c.1095C>G	p.P365P	LBD	aberrant splicing	(Wright, et al., 2004)
intron 7	c.1101-1G>A	n.d.	n.a.	skipping of exon 8	(Audo, et al., 2008)
exon 7	c.1112T>G	p.L371W	LBD/h10h11	no dimerization	(Ripamonti, et al., 2014)
exon 8	c.1120C>T	p.L374F	LBD/h10h11	no dimerization	(Cima, et al., 2012)
exon 8	c.1154G>C	p.R385P	LBD/h10h11	impaired dimerization	(Haider, et al., 2000)
exon 8	c.1217A>G[f]	p.D406G	LBD/h10h11	impaired dimerization	(Manayath, et al., 2014)
exon 8	c.1220T>A	p.M407K	LBD/h10h11	impaired dimerization	(Haider, et al., 2000)

[a]Variants are numbered in accordance to the GenBank entry NM_014249.2, where +1 corresponds to the A of the ATG translation initiation codon, *i.e.* nucleotide 191. For intronic sequences, human chromosome 15 sequence NCBI 36:15 was used. [b]Amino acid changes are numbered in accordance to the SwissProt entry Q9Y5X4. [c]The predicted effects and *in vitro* studies are discussed in the main text. [d]This variant was initially repored as p.C67_G69del. [e]This mutation was initially reported as p.E341K. [f]This variant was initially reported as c.1117A>G. n.d.: not determined; n.a.: not appropriate. A list of all published *NR2E3* sequence variants is available on www.lovd.nl/eye.

Supp. Table S3. Summary of functional studies on NR2E3 LBD variants

Variant	NR2E3	CRX	NRL	NR1D1	Rhodopsin	M-opsin
WT	+	+	+	+	+	+
W234S	++	+	+	-	+	+
A256E	+(+)	+	+	+	-	+
A256V	+	+	+	+	+	+
L263P	-	+	+	+	+	-
R309G	+	+	+	+	+	+
R311Q	+	+	+	+	+(+)	+
R334G	+	+	+	+	+	+
L336P	--	+	-	-	-	-
L353V	--	+	-	-	-	-
R385P	--	+	-	-	+(+)	+
M407K	-	+	+	+	+	+

Missense variants of the NR2E3 LBD (Variant) were tested by $BRET^2$ assays for the ability to form NR2E3 homodimers (NR2E3) and to heterodimerize with CRX, NRL and NR1D1. Transactivation studies tested for the ability of NR2E3 LBD variants to activate the rhodopsin promoter and to repress the M-opsin promoter. + sign corresponds to an activity comparable to the NR2E3 wild-type protein, and +(+), ++, - and -- signs indicate significant increases and decreases in activity.

Supp. References

Audo I, Michaelides M, Robson AG, Hawlina M, Vaclavik V, Sandbach JM, Neveu MM, Hogg CR, Hunt DM, Moore AT and others. 2008. Phenotypic variation in enhanced S-cone syndrome. Invest. Ophthalmol. Vis. Sci. 49(5):2082-2093.

Bandah D, Merin S, Ashhab M, Banin E, Sharon D. 2009. The spectrum of retinal diseases caused by *NR2E3* mutations in Israeli and Palestinian patients. Arch. Ophthalmol. 127(3):297-302.

Bernal S, Solans T, Gamundi MJ, Hernan I, de Jorge L, Carballo M, Navarro R, Tizzano E, Ayuso C, Baiget M. 2008. Analysis of the involvement of the *NR2E3* gene in autosomal recessive retinal dystrophies. Clin. Genet. 73(4):360-366.

Cassiman C, Spileers W, De Baere E, de Ravel T, Casteels I. 2013. Peculiar fundus abnormalities and pathognomonic electrophysiological findings in a 14-month-old boy with NR2E3 mutations. Ophthalmic Genet. 34(1-2):105-108.

Cima I, Brecelj J, Sustar M, Coppieters F, Leroy BP, De Baere E, Hawlina M. 2012. Enhanced S-cone syndrome with preserved macular structure and severely depressed retinal function. Doc. Ophthalmol. 125(2):161-168.

Collin RW, van den Born LI, Klevering BJ, de Castro-Miró M, Littink KW, Arimadyo K, Azam M, Yazar V, Zonneveld MN, Paun CC and others. 2011. High-resolution homozygosity mapping is a powerful tool to detect novel mutations causative of autosomal recessive RP in the Dutch population. Invest. Ophthalmol. Vis. Sci. 52(5):2227-2239.

Coppieters F, Leroy BP, Beysen D, Hellemans J, De Bosscher K, Haegeman G, Robberecht K, Wuyts W, Coucke PJ, De Baere E. 2007. Recurrent mutation in the first zinc finger of the orphan nuclear receptor *NR2E3* causes autosomal dominant retinitis pigmentosa. Am. J. Hum. Genet. 81:147-157.

Haider NB, Jacobson SG, Cideciyan AV, Swiderski R, Streb LM, Searby C, Beck G, Hockey R, Hanna DB, Gorman S and others. 2000. Mutation of a nuclear receptor gene, NR2E3, causes enhanced S cone syndrome, a disorder of retinal cell fate. Nat. Genet. 24(2):127-131.

Hayashi T, Gekka T, Goto-Omoto S, Takeuchi T, Kubo A, Kitahara K. 2005. Novel NR2E3 mutations (R104Q, R334G) associated with a mild form of enhanced S-cone syndrome demonstrate compound heterozygosity. Ophthalmology 112(12):2115.

Kannabiran C, Singh H, Sahini N, Jalali S, Mohan G. 2012. Mutations in TULP1, NR2E3, and MFRP genes in Indian families with autosomal recessive retinitis pigmentosa. Mol. Vis. 18:1165-1174.

Khan AO, Aldahmesh MA, Al-Harthi E, Alkuraya FS. 2010. Helicoid subretinal fibrosis associated with a novel recessive NR2E3 mutation p.S44X. Arch. Ophthalmol. 128(3):344-348.

Kuniyoshi K, Hayashi T, Sakuramoto H, Nakao A, Sato T, Utsumi T, Tsuneoka H, Shimomura Y. 2013. Novel mutations in enhanced S-cone syndrome. Ophthalmology 120(2):431.e1-6.

Lam BL, Goldberg JL, Hartley KL, Stone EM, Liu M. 2007. Atypical mild enhanced S-cone syndrome with novel compound heterozygosity of the *NR2E3* gene. Am. J. Ophthalmol. 144(1):157-159.

Manayath GJ, Namburi P, Periasamy S, Kale JA, Narendran V, Ganesh A. 2014. A novel mutation in the NR2E3 gene associated with Goldmann-Favre syndrome and vasoproliferative tumor of the retina. Mol. Vis. 20:724-731.

Nakamura Y, Hayashi T, Kozaki K, Kubo A, Omoto S, Watanabe A, Toda K, Takeuchi T, Gekka T, Kitahara K. 2004. Enhanced S-cone syndrome in a Japanese family with a nonsense NR2E3 mutation (Q350X). Acta Ophthalmol. Scand. 82(5):616-622.

Pachydaki SI, Klaver CC, Barbazetto IA, Roy MS, Gouras P, Allikmets R, Yannuzzi LA. 2009. Phenotypic features of patients with NR2E3 mutations. Arch. Ophthalmol. 127(1):71-75.

Park SP, Hong IH, Tsang SH, Lee W, Horowitz J, Yzer S, Allikmets R, Chang S. 2013. Disruption of the human cone photoreceptor mosaic from a defect in NR2E3 transcription factor function in young adults. Graefes Arch. Clin. Exp. Ophthalmol. 251(10):2299-2309.

Ripamonti C, Aboshiha J, Henning GB, Sergouniotis PI, Michaelides M, Moore AT, Webster AR, Stockman A. 2014. Vision in observers with enhanced S-cone syndrome: an excess of s-cones but connected mainly to conventional s-cone pathways. Invest. Ophthalmol. Vis. Sci. 55(2):963-976.

Rocha-Sousa A, Hayashi T, Gomes NL, Penas S, Brandão E, Rocha P, Urashima M, Yamada H, Tsuneoka H, Falcão-Reis F. 2011. A novel mutation (Cys83Tyr) in the second zinc finger of NR2E3 in enhanced S-cone syndrome. Graefes Arch. Clin. Exp. Ophthalmol. 249(2):201-208.

Sharon D, Sandberg MA, Caruso RC, Berson EL, Dryja T. 2003. Shared mutations in *NR2E3* in enhanced S-cone syndrome, Goldmann-Favre syndrome, and many cases of clumped pigmentary retinal degeneration. Arch. Ophthalmol. 121:1316-1323.

Siemiatkowska AM, Arimadyo K, Moruz LM, Astuti GD, de Castro-Miro M, Zonneveld MN, Strom TM, de Wijs IJ, Hoefsloot LH, Faradz SM and others. 2011. Molecular genetic analysis of retinitis pigmentosa in Indonesia using genome-wide homozygosity mapping. Mol. Vis. 17:3013-3024.

Tan MH, Zhou XE, Soon FF, Li X, Li J, Yong EL, Melcher K, Xu HE. 2013. The crystal structure of the orphan nuclear receptor NR2E3/PNR ligand binding domain reveals a dimeric auto-repressed conformation. PLoS One 8(9):e74359.

Udar N, Small K, Chalukya M, Silva-Garcia R, Marmor M. 2011. Developmental or degenerative--NR2E3 gene mutations in two patients with enhanced S cone syndrome. Mol. Vis. 17:519-525.

Wright AF, Reddick AC, Schwartz SB, Ferguson JS, Aleman TS, Kellner U, Jurklies B, Schuster A, Zrenner E, Wissinger B and others. 2004. Mutation analysis of NR2E3 and NRL genes in enhanced S-cone syndrome. Hum. Mutat. 24(5):439-450.